This is the Pre-Published Version.

This document is the Accepted Manuscript version of a Published Work that appeared in final form in Energy & Fuels, copyright © 2024 American Chemical Society after peer review and technical editing by the publisher. To access the final edited and published work see https://doi.org/10.1021/acs.energyfuels.4c03034.

Performance characteristics of a H_2O_2-based fuel cell under extreme environments

Xingyi Shi[#, 1, 3], Yuran Bai[#, 1], Xiaoyu Huo[1], Yun Liu[1], Lizhen Wu[1], Wenzhi Li[1], Qixing Wu*[, 2], Liang An*[, 1, 3]

[1] Department of Mechanical Engineering, The Hong Kong Polytechnic University, Hung Hom, Kowloon, Hong Kong SAR, 999077, China

[2] Shenzhen Key Laboratory of New Lithium-ion Batteries and Mesoporous Materials, College of Chemistry and Environmental Engineering, Shenzhen University, Shenzhen, 518060, Guangdong Province, China

[3] Research Institute for Smart Energy, The Hong Kong Polytechnic University, Hung Hom, Kowloon, Hong Kong SAR, 999077, China.

[#] These authors contributed equally to this work.

* Corresponding authors.

Email: qxwu@szu.edu.cn (Q. Wu)

Email: liang.an@polyu.edu.hk (L. An)

Abstract

In recent decades, the liquid fuel cell has attracted considerable interest due to its inherent advantages, including simple design, almost instantaneous rechargeability and high energy density. However, despite these merits, hampered by the slow reaction kinetics of alcoholic liquid fuels, their cell performances remain inadequate even with the assistance of noble metal catalysts. As an alternative, a novel electrically rechargeable liquid fuel (e-fuel) has recently been proposed and is found to exhibit a

significantly improved cell performance presenting it to be with great potential for widespread use. Nevertheless, before realizing its commercialization, it is a prerequisite for the fuel cell to be operational under extreme conditions, such as air-free and low-temperature environment. In this work, fed with the e-fuel and hydrogen peroxide, a passive fuel cell is designed and fabricated. The impacts of operating temperature on the properties of cell components are studied, while the effects of diverse operating conditions on the cell performance are investigated. The cell is found to be able of reaching a peak power density of 31.7 mW cm^{-2} even at -20 ºC without any cold-start strategies. Furthermore, it is also proven capable of achieving stable operation without auxiliary equipment. This impressive performance especially under extreme operating conditions demonstrates the remarkable potential of this present system for applications in the future.

Keywords: E-fuel; Extreme conditions, Air-free, Sub-zero environment; Liquid fuel cell

1. Introduction

The achievement of sustainable development and carbon neutrality is an essential goal for modern society, which requires promoting the widespread use of renewable energy sources[1, 2]. Among diverse kinds of renewable power systems, the hydrogen-oxygen fuel cell with its high efficiency and zero emission is regarded as a promising candidate[3, 4]. However, hampered by the significant safety risks during the handling of gaseous hydrogen, the world-wide adoption of the hydrogen fuel cell still faces many challenges[5]. As a potential alternative, liquid fuel cells, powered using alcoholic fuels (e.g., methanol), have attracted much attentions[6]. The substitution of gaseous hydrogen with liquid fuels facilitated the fuel handling and increased the system energy density, while the cell performance is greatly impeded by the sluggish reaction kinetics of conventional alcoholic liquid fuels[7]. Consequently, aiming to further enhance the liquid fuel cell performances, it is essential to identify alternative liquid fuels with better reactivity.

In recent years, a new type of electrically rechargeable liquid fuel, known as e-fuel, has been demonstrated to attain superior cell performances under diverse operating conditions, presenting significant potential for a variety of applications[8]. Before realizing its commercialization, however, it is essential for the e-fuel cell to be operational under extreme conditions, such as air-free and low operating temperature, especially in confined spaces[9]. As the limited space prohibits the use of auxiliary equipment, including: oxygen cylinders, heaters, and thermal control systems, the ability of the e-fuel cell to operate stably and independently under extreme conditions

is of vital importance[10]. Furthermore, easily influenced by the operating condition, the practical performances of fuel cells always tend to get severely compromised in harsh environments such as arctic expeditions and underwater explorations[11-13].

Operation of a fuel cell typically requires an oxidant at the cathode, where gaseous oxygen and ambient air are the most frequent choices[14]. Whilst it is a preferred choice, in special application scenarios, such as outer space and deep-sea environments, an alternative oxidant is required to substitute the gaseous oxygen[15, 16]. Hydrogen peroxide, as a promising replacement possesses many unique advantages including: i) help avoiding the water flooding problem with its intrinsic liquid phase; and ii) reduce the activation losses with its fast reaction kinetics due to the two-electron-transfer process[17, 18]. Besides the oxidant, the operating temperature is another major factor determining the cell performances, particularly at low temperature environment (< 0°C). The low operating temperature not only hinders the reaction kinetics of reactive species, but also restrains their mobility, thereby leading to large polarization losses and limiting the cell output performances[11]. Conventionally, cold-start techniques such as pre-heating are required to enable the operation of fuel cells in sub-zero environments, where auxiliary equipment such as heaters are needed[19, 20]. Yet, the involvement of such procedure and devices results in a complicated system structure and deteriorates the system energy density and efficiency[21]. Thus, prior to the wide utilization of fuel cells, it is imperative to develop a fuel cell capable of operating independently and continuously under extreme conditions, including air-free and sub-zero operating temperature.

In this study, to enable a stable power generation under extreme conditions, a hydrogen

peroxide-based passive e-fuel fuel cell has been developed. Firstly, the e-fuel, oxidant, and membrane properties, including conductivities and viscosities, are investigated at different temperatures. Then, the study analyzed the influences of various operating conditions on the cell performances, including current collector designs, e-fuel and oxidant compositions, and operating temperatures. Overall, by substituting gaseous oxygen with liquid oxidant (hydrogen peroxide), the passive fuel cell has reached a peak power density (PPD) of 72.9 mW cm^{-2}. More impressively, even at -20 °C, a PPD of 31.7 mW cm^{-2} is attained without any cold-start process. Such superior cell performance thus demonstrates its resilience and flexibility to operate under extreme conditions, thereby highlighting its enormous potential for future applications.

2. Working principle

The structure of the liquid e-fuel cell is as shown in Fig. 1 (a). At either side of the e-fuel cell, a pair of tanks is equipped for storing the liquid e-fuel and hydrogen peroxide, respectively. During cell operation, on the anode side, the V(II) ions are oxidized to V(III) while the electrons being released following the electrochemical reaction as shown in equation (1):

$$V^{2+} - e^- \rightarrow V^{3+} \qquad E_0^a = -0.26V \tag{1}$$

Meanwhile, at the cathode side, the hydrogen peroxide undergoes the reduction reaction as in equation (2):

$$\frac{1}{2}H_2O_2 + H^+ + e^- \rightarrow H_2O \qquad E_c^0 = 1.78\,V \tag{2}$$

The overall reaction thus can be derived as in equation (3):

$$2V^{2+} + H_2O_2 + 2H^+ \rightarrow 2V^{3+} + 2H_2O \qquad E^0 = 2.04V \tag{3}$$

In comparison to the conventional gaseous oxygen (1.49 V)[22], the hydrogen peroxide, as a substitute enables the e-fuel cell with a higher theoretical voltage of 2.04 V, thereby greatly increasing the system energy density.

3. Experiments

3.1 Preparation of a membrane electrode assembly

In this e-fuel cell, the membrane electrode assembly used was with an effective area of 2.0 × 2.0 cm. The commercial graphite felt (Liaoning Jingu Carbon Material) was used as the anode directly without any further treatments, while the homemade Pt/C coated carbon paper was used as the cathode with a Pt loading of 0.5 mg cm^{-2}.[23] The Nafion 115 membrane was pretreated as reported before being further used[23].

3.2 E-fuel cell setup and instrumentation

The passive e-fuel cell (Fig. 1 (a)) was composed of a titanium cathode current collector, a graphite anode current collector, and a pair of acrylic tanks and stainless-steel endplates. The anode graphite current collector adopts the rectangular parallel channels design with an open ratio of 70%, which is as reported before[24]. To prevent the leakage of fuels and oxidants, multiple pieces of gaskets were also employed during the cell assembling. The oxidant was fabricated by mixing the hydrogen peroxide (30%, VWR) with sulfuric acid (Honeywell, Fluka) to obtain the desired composition. While the e-fuel was prepared by first dissolving the vanadyl sulfate into the sulfuric acid and then charged using a conventional flow cell before being fed into the cell for further studies[25]. The experimental setup was illustrated in Fig. 1 (b), which includes a cell, a low-temperature test chamber, a thermocouple, and a fuel cell testing system for evaluating the cell performance. The cyclic voltammetry (CV) test was performed using a three-

electrode cell, which includes a working electrode (graphite felt, 1.0 cm × 1.0 cm), a counter electrode (platinum wire), and a reference electrode (Ag/AgCl). It is worth noting that, to avoid the freezing issue of the reference electrode at sub-zero environment, the saturated potassium chloride solution was mixed with the ethylene glycol before being filled into the reference electrode, which is as reported previously[26]. The electrolyte filled into the three-electrode cell during CV tests was composed of 0.1 M V(II) in 4.0 M H_2SO_4. Using the same set-up, the linear sweep voltammetry test was conducted for examining the cathode performances, where the electrolyte was consisted of 0.5 M H_2O_2 in 4.0 M H_2SO_4 while the 1.0 cm × 1.0 cm Pt/C coated carbon paper is served as the working electrode. To measure the membrane conductivity, the electrochemical impedance spectroscopy (EIS) test was performed at 0.01 to 10^5 Hz, where the Nafion 115 membrane was clamped by a pair of stainless-steel plates. After the impedance was obtained, the membrane conductivity was then calculated with the equation as in equation (4)[11]:

$$\sigma_m(\mathrm{S\ cm^{-1}}) = \frac{t}{R_m S} \tag{4}$$

where t and S stand for the membrane thickness and membrane effective area, respectively. R_m is the membrane resistance, which came from the Nyquist plots. As reported previously, the e-fuel and oxidant conductivities were also tested through the EIS[11], while their viscosities at low-temperature environment were tested using the Ubbelohde viscometer. The CV, LSV and EIS tests was all performed with an electrochemical workstation (CHI-660e, CH Instruments, China). It is worth noting that, before starting tests, the set-up was pre-cooled using the low-temperature chamber to

reach the target operating temperature.

4. Results and discussion

4.1 E-fuel and hydrogen peroxide performances

The chemical compositions of the e-fuel and the oxidant determine their inherent properties, such as their viscosities and ionic conductivities[27]. The operating temperature, in the meanwhile, also plays a crucial role in influencing these properties, which further affects the cell performance. By adding with sulfuric acid, the e-fuel and hydrogen peroxide are granted with a low frozen point, thereby enabling them to operate at sub-zero temperatures. Therefore, the viscosities and conductivities of the e-fuel and oxidant are first examined at -20 to 20 °C (Fig. 2(a)). A decrease in operating temperature has been observed to result in an increase in the viscosities of both e-fuel and oxidant. It can be attributed to the reduced kinetic energy limiting the movement of ions and water molecules[28, 29], which consequently leads to the decrement of ionic conductivities, thus demonstrating the great impact of operating temperature on the e-fuel and oxidant properties.

4.2 Membrane performance

The proton exchange membrane as a critical component within the fuel cell, functions as a conduction channel between anode and cathode[30]. Its primary role is to facilitate the transport of protons while blocking the crossover of e-fuels and oxidants. Therefore, it is vital for the membrane to possess high proton conductivity, so as to enable fast transport of protons from one side to the other, thereby lowering the ohmic polarization loss. Nevertheless, while membrane properties significantly affect the fuel cell performance, its conductivity is readily influenced by operating temperature. Hence,

the membrane conductivity is measured at different operating temperatures (Fig. 2 (b)). As can be seen that, with the temperature decreases to -20 °C, the membrane conductivity drops from 19.57 to 10.40 mS cm^{-1}. Such a decline in membrane conductivity can be mainly attributed to two factors: i) according to the hopping mechanism, the increased difficulty for protons to escape from hydronium ions at low temperature hinders the proton transfer process; and ii) according to the vehicular mechanism, the diffusion process of water molecules, which act as carriers of the protons, slows down at low temperature, thereby hindering the mobility of the protons[31]. Thus, overall, the membrane conductivity gets lower as the operating temperature falls. In addition to the membrane conductivity, it should also be noted that, the decline of operating temperature would on the other hand impede the crossover of fuel and oxidants through the membrane, which thereby would reduce fuel losses during the cell operation.

4.3 Electrode performance

CV is a widely used diagnostic method for examining the electrochemical performance of electrodes. Hence, in this work, CV tests are carried out to analyze the effects of operating temperatures on the anode performances as shown in Fig. 3 (a). It is found that, as temperature decreases, the peak current drops while the peak potential separation increases from 323 mV (20 °C) to 567 mV (-20 °C), demonstrating the slowed reaction kinetics of the e-fuel[32]. Such an apparent performance degradation is also related to the high e-fuel viscosity at low operating temperature hampering the diffusion process of reactive species to reach the reactive site on the electrode surface. Meanwhile, using the linear sweep voltammetry (LSV) test, the cathode performance

is also examined at different temperatures. As shown in Fig. 3 (b), with the operating temperature decreases, the current density also shows an obvious downward trend with a gradually weakened current density peak, indicating the declined reaction kinetics of the oxidant reduction reaction. Nonetheless, both the e-fuel and the oxidant are found to possess electrochemical reactivity even at -20 °C, presenting them to be with capability for power generation in sub-zero environments.

4.4 Effect of the current collector designs

The design of the current collector has a crucial impact on the fuel cell performance. It not only provides channels for supplying the fuel and oxidant, but also collects the electrons and acts as a support for the electrode. Thus, it is necessary for the current collector to possesses good electrical conductivity, high mechanical strength and ease of supply of reactants[24]. On the cathode side, since the oxidant (hydrogen peroxide) would inevitably undergo self-decomposition reaction, it is also necessary for the current collector design to provide pathways to facilitate the escape of bubbles generated[33]. In this work, six types of different current collector designs are adopted for the cathode and named as shown in Fig. 4 (a). Among these current collectors, CC-1, CC-3, and CC-5 use the conventional parallel design, while CC-2, CC-4, and CC-6 apply the perpendicular design to ease the exit of bubbles. By assembling these current collectors into the fuel cell, the cell using the parallel design current collectors (CC-1, CC-3 and CC-5) is found to show a much lower maximum current density than the cell with the perpendicular design current collectors (CC-2, CC-4, and CC-6), even though they have the same open ratio. Such an obvious performance difference is caused by the difficulty for bubble to escape, thereby confining the effective surface area for

electrochemical reactions and restricting the mass transport process of reactants[34]. Meanwhile, for the current collectors with the perpendicular design, the fuel cell performance is found to improve as the open ratio increases. Specifically, the PPD of the cell rises from 40.4 to 72.9 mW cm^{-2} as the current collector open ratio increase from 70 % (CC-2) to 90 % (CC-6). Hence, CC-6 with the best power output is used for the following tests. It is also worth noting that, while a high open ratio of the current collector can improve the cell performance, further increment of the current collector open ratio could induce large ohmic resistance and influences the electrode integrity especially after long-term operation.

4.5 Effect of the oxidant composition

Hydrogen peroxide, as a well-known replacement to the gaseous oxygen, allows the fuel cell to operate in an oxygen-free environment[35]. Meanwhile, the sulfuric acid, acting as the supporting electrolyte, not only provides reactive species to participate in the electrochemical reaction, but also stabilize the H_2O_2 to avoid self-decomposition reactions[36]. Therefore, the composition of the oxidant is believed to significantly influence the fuel cell performance and is thoroughly examined here. To begin with, the effects of H_2O_2 concentration is studied. As shown in Fig. 5(a), with the hydrogen peroxide concentration increases from 1.0 M to 5.0 M, the PPD also increases, which is due to the availability of more reactants for the electrochemical reaction at the reaction site, thereby lowering the concentration polarization losses. However, as the hydrogen peroxide concentration further raises to 7.0 M, the PPD begins to decrease, which is resulting from the competitive absorption between hydrogen peroxide and protons limiting the supply of hydrogen peroxide. In addition, such a high concentration

of hydrogen peroxide could also result in a more severe crossover issue, which could induce mixed potential and further deteriorate the cell performance. Similarly, for the sulfuric acid concentration, the optimum concentration is identified to be 4.0 M. A higher H_2SO_4 concentration than 4.0 M would induce competitive absorption and a high electrolyte viscosity, hindering the transport of reactive species. While a lower H_2SO_4 concentration would result in lack of protons to participate in the cathodic electrochemical reactions, thereby leading to a large activation polarization loss. Notably, the cell PPD only reaches 26.8 mW cm^{-2} when no sulfuric acid is added into the oxidant electrolyte. Overall, the oxidant with 5.0 M H_2O_2 in 4.0 M H_2SO_4 is found to be the optimal choice with a PPD of 72.9 mW cm^{-2}.

4.6 Effect of the operating temperature

As demonstrated in previous sections, the operating temperature significantly impacts the properties of cell components, including the membrane, electrodes, fuel and oxidant. Hence, in this section, the effects of operating temperature on the cell performance is examined (Figure 6)[37]. It can be seen that, as the temperature declines from 20 to -20 ºC, the PPD also drops from 72.9 to 31.7 mW cm^{-2}. Such a trend, on the one hand, is aroused from the high activation loss at low operating temperature. As proved by the CV and LSV results in the previous section, the reaction kinetics of the cathodic and anodic electrochemical reactions decrease significantly with the operating temperature gets lower. On the other hand, the degraded cell performance is aroused from the increased ohmic losses, which is induced by the high membrane, e-fuel and oxidant impedances. Furthermore, influenced by the high fuel and oxidant viscosities, the lowered operating temperature also hinders the mass transport process of reactive

species thereby leading to a high mass transport loss. Nevertheless, the cell is able to deliver a PPD of 31.7 mW cm^{-2} at -20 ºC, even without any cold-start strategies, making it a preferable choice for applications in extreme conditions.

4.7 Constant-current discharging behavior and demonstration

The constant-current discharging behavior is an important test to assess the fuel cell performances before implementing wide applications. Hence, as presented in Fig. 7 (a), the performance of the e-fuel cell is studied at 20 to -20 °C. As the operating temperature decreases, both the discharging voltage plateau and operation duration of the e-fuel cell reduce significantly. The reduction on discharging voltage plateau is attributed to the increase in polarization losses, which thus limits the voltage output. While the low discharge duration is aroused from the earlier hit of the cut-off voltage, thereby limiting the usage of reactive species. It is worth noting that, the high viscosity of e-fuel and oxidant at low operating temperature is another cause for confining the cell discharging performance, as it restricts the mass transport process thereby limiting the supply of reactive species. To further present the applicability of this system under extreme conditions, the e-fuel cell is also used for powering the LED lights at -20 °C demonstrating its potential for usage in real-life scenarios (Fig. 7 (b)).

5. Conclusion

In this work, a passive fuel cell, fed with the e-fuel and hydrogen peroxide has been designed and fabricated. The influences of operating temperatures on the cell component properties and cell performances are explored, while the optimal current collector design and oxidant composition are identified. The cell is found to attain a PPD of 72.9 mW cm^{-2} in an oxygen-free environment. Even at -20 °C, a PPD of 31.7

mW cm^{-2} is attained without the assistance of any heating devices. The successful demonstration of the presented fuel cell not only broadens its application scenarios, but also presents it to be with a huge potential for widespread applications, especially under extreme conditions. However, before realizing its commercialization, further performance advancement is still essential. For instance, it is necessary to develop membranes with higher proton conductivity especially at sub-zero environment to enable a faster proton transport process inside, thereby granting the system with better performance at sub-zero environment.

Conflicts of interest

There are no conflicts to declare.

Acknowledgement

The work described in this paper was supported by a grant from the National Natural Science Foundation of China (No. 52076142), a grant from the NSFC/RGC Joint Research Scheme (N_PolyU559/21), and a grant from Research Institute for Smart Energy at The Hong Kong Polytechnic University (CDB2).

References

1. Chen, X.; Zhou, W., Support carbon neutrality target—Which flexible power source is the best option for China? *Energy* **2023,** *285*, 128682.
2. Erdogan, S.; Pata, U. K.; Solarin, S. A., Towards carbon-neutral world: The effect of renewable energy investments and technologies in G7 countries. *Renew. Sust. Energ. Rev.* **2023,** *186*, 113683.
3. Shi, X.; Ma, Y.; Huo, X.; Esan, O. C.; An, L., Nafion membranes for e-fuel cell

applications. *Int. J. Green Energy* **2021**, 1-7.
4. Haider, R.; Wen, Y.; Ma, Z.-F.; Wilkinson, D. P.; Zhang, L.; Yuan, X.; Song, S.; Zhang, J., High temperature proton exchange membrane fuel cells: progress in advanced materials and key technologies. *Chemical Society Reviews* **2021,** *50* (2), 1138-1187.
5. Schlapbach, L., Hydrogen-fuelled vehicles. *Nature* **2009,** *460* (7257), 809-811.
6. Shaari, N.; Kamarudin, S. K.; Bahru, R.; Osman, S. H.; Md Ishak, N. A. I., Progress and challenges: Review for direct liquid fuel cell. *Int. J. Energy Res.* **2021,** *45* (5), 6644-6688.
7. Zheng, J.; Zhang, W.; Zhang, J.; Lv, M.; Li, S.; Song, H.; Cui, Z.; Du, L.; Liao, S., Recent advances in nanostructured transition metal nitrides for fuel cells. *J. Mater. Chem. A* **2020,** *8* (40), 20803-20818.
8. Shi, X.; Huo, X.; Esan, O. C.; Pan, Z.; Yun, L.; An, L.; Zhao, T., Mathematical modeling of fuel cells fed with an electrically rechargeable liquid fuel. *Energy and AI* **2023,** *14*, 100275.
9. Chen, M.; Zhang, Y.; Xing, G.; Chou, S.-L.; Tang, Y., Electrochemical energy storage devices working in extreme conditions. *Energy Environ. Sci.* **2021,** *14* (6), 3323-3351.
10. Massaro, M. C.; Biga, R.; Kolisnichenko, A.; Marocco, P.; Monteverde, A. H. A.; Santarelli, M., Potential and technical challenges of on-board hydrogen storage technologies coupled with fuel cell systems for aircraft electrification. *J. Power Sources* **2023,** *555*, 232397.
11. Shi, X.; Huo, X.; Esan, O. C.; Ma, Y.; An, L.; Zhao, T., A liquid e-fuel cell operating at− 20° C. *J. Power Sources* **2021,** *506*, 230198.
12. Wang, X.; Baker, P.; Zhang, X.; Garces, H. F.; Bonville, L. J.; Pasaogullari, U.; Molter, T. M., An experimental overview of the effects of hydrogen impurities on polymer electrolyte membrane fuel cell performance. *Int. J. Hydrogen Energy* **2014,** *39* (34), 19701-19713.
13. Ozen, D. N.; Timurkutluk, B.; Altinisik, K., Effects of operation temperature and reactant gas humidity levels on performance of PEM fuel cells. *Renew. Sust. Energ. Rev.* **2016,** *59*, 1298-1306.
14. Cigolotti, V.; Genovese, M.; Fragiacomo, P., Comprehensive review on fuel cell technology for stationary applications as sustainable and efficient poly-generation energy systems. *Energies* **2021,** *14* (16), 4963.
15. Oh, T. H., Design specifications of direct borohydride–hydrogen peroxide fuel cell system for space missions. *Aerosp. Sci. Technol.* **2016,** *58*, 511-517.
16. Lao, S. J.; Qin, H. Y.; Ye, L. Q.; Liu, B. H.; Li, Z. P., A development of direct hydrazine/hydrogen peroxide fuel cell. *J. Power Sources* **2010,** *195* (13), 4135-4138.
17. Miley, G. H.; Luo, N.; Mather, J.; Burton, R.; Hawkins, G.; Gu, L.; Byrd, E.; Gimlin, R.; Shrestha, P. J.; Benavides, G., Direct NaBH4/H2O2 fuel cells. *J. Power Sources* **2007,** *165* (2), 509-516.
18. Sanli, A.; Aytaç, A., Response to Disselkamp: direct peroxide/peroxide fuel cell as a novel type fuel cell. *Int. J. Hydrogen Energy* **2011,** *36* (1), 869-875.
19. Hu, X.; Zheng, Y.; Howey, D. A.; Perez, H.; Foley, A.; Pecht, M., Battery warm-up

methodologies at subzero temperatures for automotive applications: Recent advances and perspectives. *Progr. Energy Combust. Sci.* **2020,** *77*, 100806.
20. Atanassov, P., Fuel Cells: A Call for Total Design. *Joule* **2018,** *2* (7), 1210-1211.
21. Luo, Y.; Jiao, K., Cold start of proton exchange membrane fuel cell. *Progr. Energy Combust. Sci.* **2018,** *64*, 29-61.
22. Shi, X.; Huo, X.; Esan, O. C.; An, L.; Zhao, T., Performance characteristics of a liquid e-fuel cell. *Appl. Energy* **2021,** *297*, 117145.
23. Shi, X.; Huo, X.; Ma, Y.; Pan, Z.; An, L., Energizing fuel cells with an electrically rechargeable liquid fuel. *Cell Rep. Phys. Sci.* **2020,** *1* (7), 1-13.
24. Shi, X.; Dai, Y.; Esan, O. C.; Huo, X.; An, L.; Zhao, T., A passive fuel cell fed with an electrically rechargeable liquid fuel. *ACS Appl. Mater. Interfaces* **2021,** *13* (41), 48795-48800.
25. Shi, X.; Huo, X.; Esan, O. C.; Dai, Y.; An, L.; Zhao, T., Manipulation of electrode composition for effective water management in fuel cells fed with an electrically rechargeable liquid fuel. *ACS Appl. Mater. Interfaces* **2022,** *14* (16), 18600-18606.
26. Yin, J.; Qi, L.; Wang, H., Antifreezing Ag/AgCl reference electrodes: fabrication and applications. *J. Electroanal. Chem.* **2012,** *666*, 25-31.
27. Xi, J.; Xiao, S.; Yu, L.; Wu, L.; Liu, L.; Qiu, X., Broad temperature adaptability of vanadium redox flow battery—Part 2: Cell research. *Electrochim. Acta* **2016,** *191*, 695-704.
28. Datta, J.; Dutta, A.; Mukherjee, S., The beneficial role of the cometals Pd and Au in the carbon-supported PtPdAu catalyst toward promoting ethanol oxidation kinetics in alkaline fuel cells: temperature effect and reaction mechanism. *J. Phys. Chem. C* **2011,** *115* (31), 15324-15334.
29. Li, X.; Xiong, J.; Tang, A.; Qin, Y.; Liu, J.; Yan, C., Investigation of the use of electrolyte viscosity for online state-of-charge monitoring design in vanadium redox flow battery. *Appl. Energy* **2018,** *211*, 1050-1059.
30. Shi, X.; Esan, O. C.; Huo, X.; Ma, Y.; Pan, Z.; An, L.; Zhao, T., Polymer electrolyte membranes for vanadium redox flow batteries: fundamentals and applications. *Progr. Energy Combust. Sci.* **2021,** *85*, 100926.
31. Deluca, N. W.; Elabd, Y. A., Polymer electrolyte membranes for the direct methanol fuel cell: a review. *J. Polym. Sci., Part B: Polym. Phys.* **2006,** *44* (16), 2201-2225.
32. Jiang, H.; Zeng, Y.; Wu, M.; Shyy, W.; Zhao, T., A uniformly distributed bismuth nanoparticle-modified carbon cloth electrode for vanadium redox flow batteries. *Appl. Energy* **2019,** *240*, 226-235.
33. Esan, O. C.; Shi, X.; Pan, Z.; Liu, Y.; Huo, X.; An, L.; Zhao, T., A high-performance H2O2-based fuel cell for air-free applications. *J. Power Sources* **2022,** *548*, 232114.
34. Zhou, Y.; Yang, Y.; Zhu, X.; Ye, D.-d.; Chen, R.; Liao, Q., Bubble-trap layer for effective removing gas bubbles and stabilizing power generation in direct liquid fuel cell. *J. Power Sources* **2021,** *507*, 230260.
35. An, L.; Zhao, T.; Li, Y.; Wu, Q., Charge carriers in alkaline direct oxidation fuel cells. *Energy Environ. Sci.* **2012,** *5* (6), 7536-7538.
36. An, L.; Zhao, T.; Zhou, X.; Wei, L.; Yan, X., A high-performance ethanol–hydrogen peroxide fuel cell. *RSC Adv.* **2014,** *4* (110), 65031-65034.

37. Zhang, N.; Chen, X.; Lu, Y.; An, L.; Li, X.; Xia, D.; Zhang, Z.; Li, J., Nano-Intermetallic AuCu3 Catalyst for Oxygen Reduction Reaction: Performance and Mechanism. *Small* **2014,** *10* (13), 2662-2669.

Figure captions

Fig. 1 (a) Fabrication and (b) experimental set-up of the passive e-fuel cell.

Fig. 2 (a) Kinematic viscosity and ionic conductivity of the liquid e-fuel and oxidant, and (b) membrane conductivity at -20 °C to 20 °C.

Fig. 3 (a) Cyclic voltammetry curves of the graphite felt anode, and (b) linear sweep voltammetry of Pt/C coated carbon paper cathode at -20 to 20 °C.

Fig. 4 (a) Design of cathode current collectors, and (b) effects of current collector design on the cell performance.

Fig. 5 Effects of (a) hydrogen peroxide concentration and (b) sulfuric acid concentration on the cell performance.

Fig. 6 Polarization and power density curves of the fuel cell at an operating temperature range from -20 ˚C to 20 ˚C.

Fig.7 (a) Constant-current discharging behavior of the e-fuel cell, and (b) lab-scale demonstration of power generation under extreme conditions.

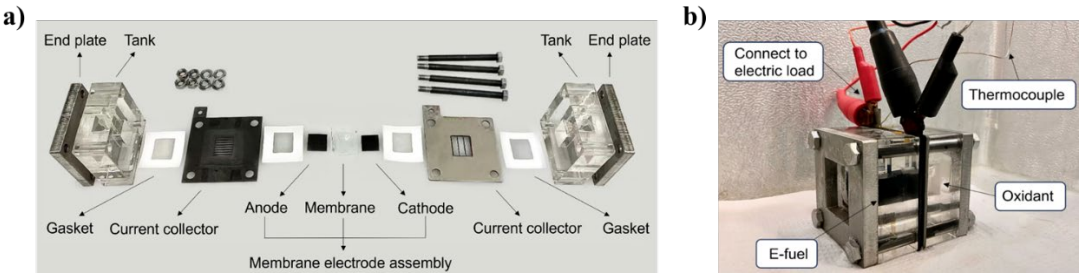

Fig. 1 (a) Fabrication and (b) experimental set-up of the passive e-fuel cell.

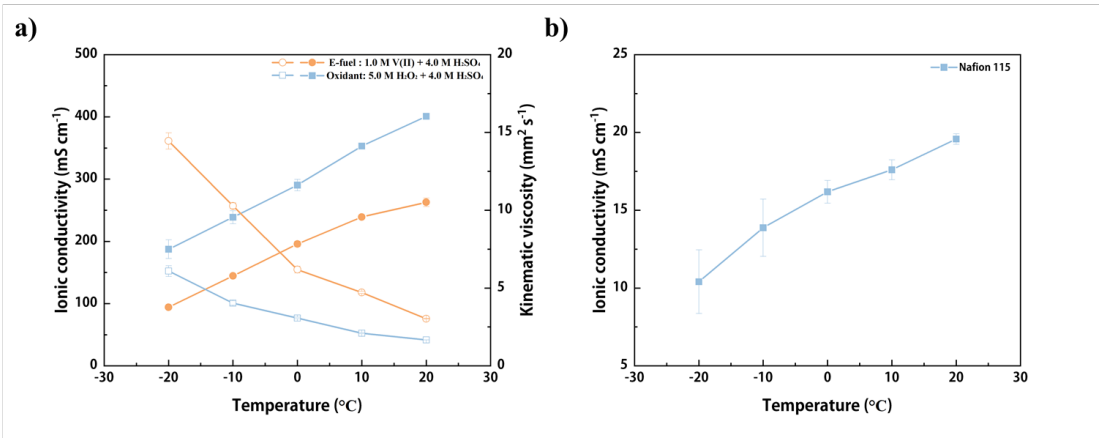

Fig. 2 (a) Kinematic viscosity and ionic conductivity of the liquid e-fuel and oxidant, and (b) membrane conductivity at -20 °C to 20 °C.

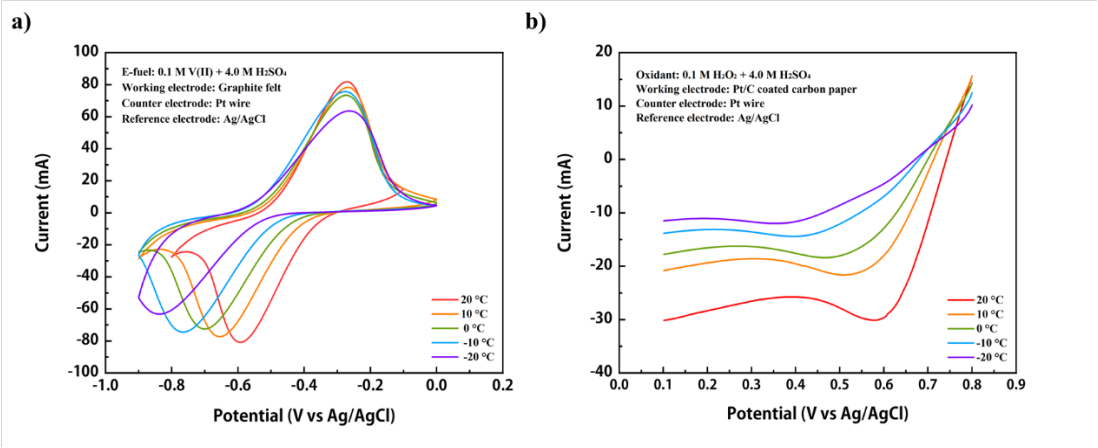

Fig. 3 (a) Cyclic voltammetry curves of the graphite felt anode, and (b) linear sweep voltammetry of Pt/C coated carbon paper cathode at -20 to 20 °C.

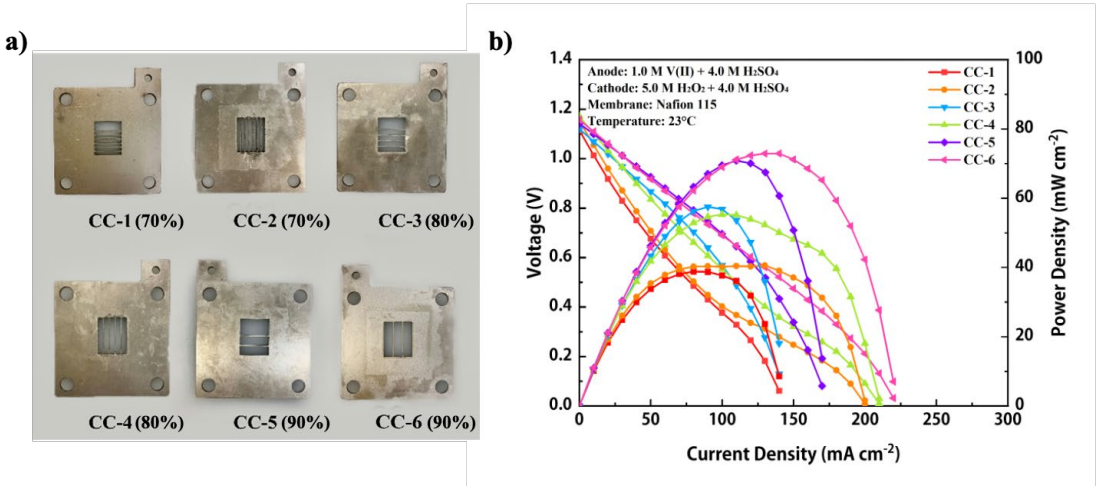

Fig. 4 (a) Design of cathode current collectors, and (b) effects of current collector design on the cell performance.

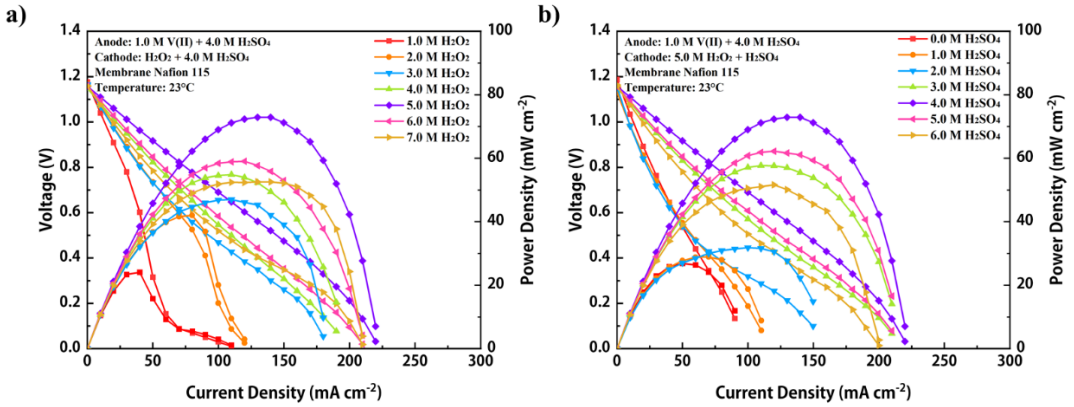

Fig. 5 Effects of (a) hydrogen peroxide concentration and (b) sulfuric acid concentration on the cell performance.

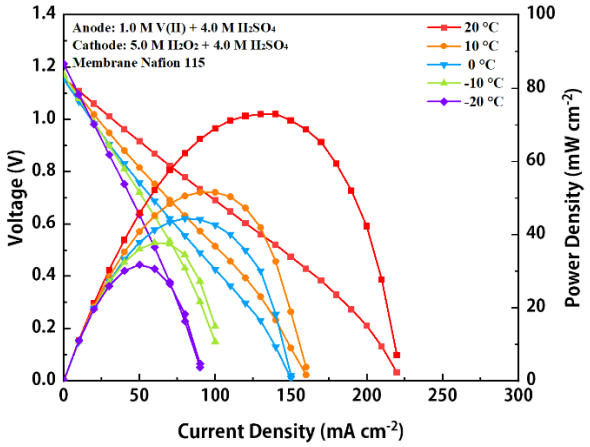

Fig. 6 Polarization and power density curves of the fuel cell at an operating temperature range from -20 ˚C to 20 ˚C.

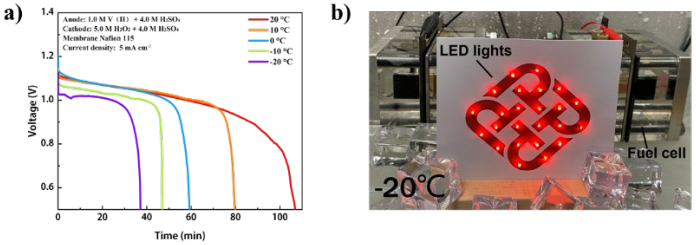

Fig.7 (a) Constant-current discharging behavior of the e-fuel cell, and (b) lab-scale demonstration of power generation under extreme conditions.

TOC graphic:

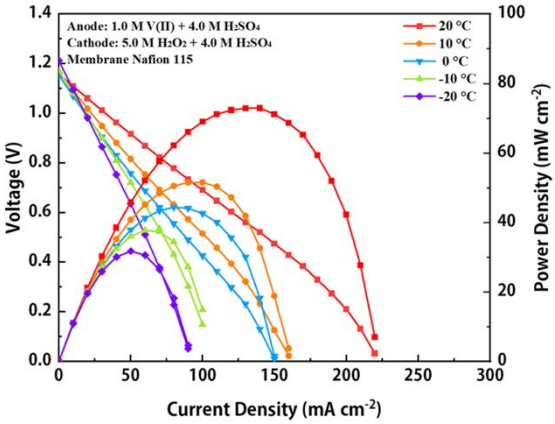
Anode: 1.0 M V(II) + 4.0 M H2SO4
Cathode: 5.0 M H2O2 + 4.0 M H2SO4
Membrane Nafion 115
20 °C
10 °C
0 °C
-10 °C
-20 °C
Voltage (V)
Power Density (mW cm-2)
Current Density (mA cm-2)

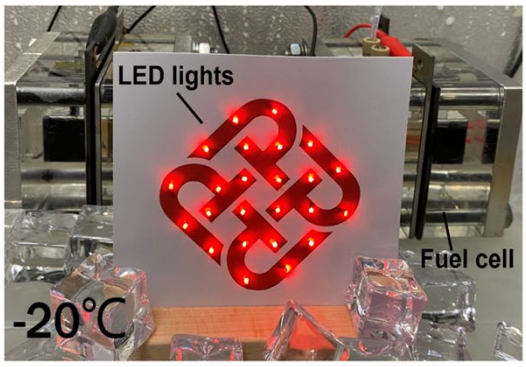
LED lights
Fuel cell
-20°C